To cite this version :

Brahim TLILI, Mustapha NASRI, F. AYARI, Corinne NOUVEAU - Fretting wear performances of multilayered PVD TiAlZrN/TiAlN/TiAl on AISI 4140 steel - International Review of Mechanical Engineering - Vol. 2, n°2, p.177-185 - 2008

Fretting Wear Performance of
Multilayered PVD TiAlZrN/TiAlN/TiAl on AISI 4140 Steel

B. Tlili[1], M. Nasri[1], F. Ayari[2], C. Nouveau[3]

Abstract – *This Nowadays, most surface treatments are realized through vapor deposition techniques as thin hard coatings to guarantee; high surface hardness, low friction coefficient and improve wear resistance. Several experimental investigations have let to the development of a (TiAlCN/TiAlN/TiAl) and (TiAlZrN/TiAlN/TiAl) coatings in preference to the traditional TiN coating. In the current paper research conducted on fretting wear of a (TiAlCN/TiAlN/TiAl) and a (TiAlZrN/TiAlN/TiAl) multilayer coatings deposited by reactive DC (magnetron sputtering) of Ti-Al and Ti-Al-Zr alloys on AISI4140 steel. Fretting wear tests (20.000 cycles at 5 Hz) were conducted in ambient conditions, where the interaction between normal load and displacement amplitude determines the fretting regime. The influence of the normal load and displacement amplitude on the coefficients of instantaneous coefficient of friction and stabilized coefficient of friction is different from the two multilayer coated steels. The PVD coating (TiAlZrN/TiAlN/TiAl) reduces the friction. The worn volume of coated AISI4140 steel is sensitive to normal load and displacement amplitude. The relation between worn volume and cumulative dissipated energy was established for the two coated steels. The energetic fretting wear coefficients were also determined. A multilayer (TiAlZrN/TiAlN/TiAl) coating has a low energetic wear coefficient.* **Copyright © 2008 Praise Worthy Prize S.r.l. - All rights reserved.**

Keywords: *Fretting wear, PVD, TiAlZrN, TiAlCN, friction coefficient, cracking, dissipated energy*

I. Introduction

The hard coatings have been used extensively to increase the wear resistance under loading conditions in fretting wear. Various methods of coating deposition have found industrial application. One successful approach is physical vapor deposition (PVD) technique. Presently, development of TiAlN based multilayer and nanocomposite coatings are the most important trends in the hard coating industry [1]. The ternary coating has better resistance to oxidation and poor adherence [2]. In order to remedy these imperfections, additional constituents such as carbon or zirconium are recommended. In order to characterize the quality of a coating, evaluation of number of properties is essential. Hardness, friction coefficient, roughness, wears and oxidation resistance have primary importance. The addition of carbon to TiAlN provides a quaternary coating, TiAlCN, which has better resistance to oxidation, improved mechanical properties and has good adherence with high Tribological capacities [3]-[4]. However, the addition of zirconium to TiAlN provides a quaternary coating, TiAlZrN. Although some studies are available on TiAlZrN layers and their behavior in terms of wear [5], data on resistance to fretting wear are not available.

Firstly, according to the intensity of the imposed parameters (normal force, amplitude of displacement and frequency) fretting maps were established to determine the sliding conditions and the type of damage according to the fretting conditions. The running condition fretting maps indicate when total or partial sliding conditions occur and the material response fretting maps quantify the damages (wear, cracking). Actually, the partial slip regime is associated with cracking as a result of a fatigue phenomenon, whereas the gross slip regime leads to wear by debris formation [6]. The mechanical models of contact including elasto-plasticity are used to delimit the boundary between partial slip and gross slip [7]. Crack propagation is studied using efficient fatigue criteria [8]-[9], while wear is studied by more or less empirical multiple quantitative approaches [10].

Secondly, in this step we have to determine the tribological properties of quaternary coatings and to correlate the worn volume according to the parameters of loading in fretting wear.

Finally, the comprehension of fretting behaviour remains sensitive as soon as the mechanical, thermal and physical-chemical interactions (occurring in a contact associated with the role played by the interfacial layer generated by detachment of the particles during friction (third body)), need to be taken into account

[12]. The third body takes part in the velocity accommodation contact mechanisms and often plays a protective role regard to the rubbing parts or first bodies [13]-[14]. The wear analysis performed with imposed displacements or tangential forces is based on an energetic approach [7], [15]. The wear volume increases linearly with the dissipated energy within the contact.

In this paper; the multilayer TiAlZrN/TiAlN/TiAl coating behaviour under various loading parameters in fretting-wear is presented.

II. Experimental Procedures

II.1. Substrate

Specimens used in this work were machined from steel trade AISI4140 hardness 420 HV0.05, with surfaces of (10x10) mm^2 and (10x12) mm^2. These samples were divided into two sets; the first set was coated by TiAlCN/TiAlN/TiAl, and the second round by TiAlZrN/TiAlN/TiAl. Before PVD treatment, all samples were cleaned and polished with trichloroethylene, acetone and alcohol in an ultrasonic cleaner.

II.2. Deposition

The multilayer coatings were deposited on the steel AISI4140 by the process of spraying DC magnetron mode. Using target compounds TiAl(50°/°Ti,50°/°Al) [3], and Al-Ti-Zr (19°/Ti°, 21°/° to Al, 10°/Zr°, 50°/°N) of high purity (99.9999%).

TABLE I
DEPOSITION CONDITIONS

Unit	Traget Power (Kw)	Bias (V)	Temper (°C)	Rotation Velocity (rpm)	Time (mn)
TiAl	6	-300	250	0.7	22
TiAlN	7.5	-200	150	0.6	17
TiAlCN	7.5	-200	100	0.6	42
TiAlZrN	7.5	-200	100	0.6	42

Unit	Ar	Gas Flow N$_2$ SCCM	C$_2$H$_2$
TiAl	400	-	-
TiAlN	770-800	90-150	-
TiAlCN	950	150-135	20-135
TiAlZrN	950	150-135	20-135

The samples were mounted on a continued rotating satellite inside the vacuum plasma chamber. The atmosphere was chosen to produce successively under a layer of TiAl, a buffer layer TiAlN then a layer of TiAlCN or TiAlZrN. Indeed, the thin films of TiAl and TiAlN aim to improve adhesion layers TiAlCN [3], [5] and TiAlZrN [11] with steel. The optimum conditions for filing as the bias voltage targets, temperature and time of deposition were determined and optimized in previous studies; Table I below shows in details the optimal conditions for verification.

In addition, Argon, acetylene and nitrogen gas are very high purity (99,999%) were introduced into the vacuum chamber. The basic pressure in the room was 5.10-5 Pa, which grows to 0.1 Pa for the deposition of desired layers. The distance between the target and the substrate surface was 35mm. Before the deposition, the surface of the substrate has been cleaned by argon ion bombardment at the end to eliminate all these antagonists.

II.3. Characterization of the Coating

The multilayer coatings prepared in this work and their mechanical properties are figured in the Table II.

TABLE II
MECHANICL PROPRIETES OF COATING LAYER AND SUBSTRATE

	Hardness (GPA)	Young's modulus (GPA)
TiAlCN/TiAlN/TiAl [3]	15	260
TiAlZrN/TiAlN/TiAl	28	310
AISI4140 STEEL	4.2	210

The fretting-wear behavior of multilayer TiAlCN/TiAlN/TiAl has been carried out in previous studies [3]. Indeed, a special focus in this paper to the characterization and the study of behaviour fretting-wear coating multilayer TiAlZrN/TiAlN/TiAl. The total thickness of the coating is determined by Electronic Scanning Microscope (SEM) after a major fracture in vertical section, followed an analysis of the chemical composition by Energy Dispersive Spectroscopy (EDS). The morphology of the coating TiAlZrN is being reviewed by an atomic force microscope (AFM). The microstructural characterization of this coating is investigated by X-ray diffraction (Philips X'pert system). Scans were carried out in the grazing angle mode with an incident beam angle of 3° and the normal θ-2θ method classically used in the same situation. Young's modulus and hardness were measured by nanoindentation tests with a nanoindenter MTS-XP. The indentation was performed using a triangular Berkovich diamond pyramid.

SEM and AFM observations allowed determination of the global coating thickness and the morphology of the surface respectively. The multilayered TiAlZrN/TiAlN/TiAl coatings had a mean thickness of 800nm distributed in three layers as shown in Fig. 1. The surface was globally uniform with some domes and tiny craters spread all over the area Fig. 2.
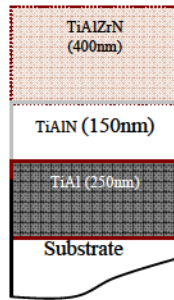
Fig. 1. Distribution and thickness of the layers in the coating
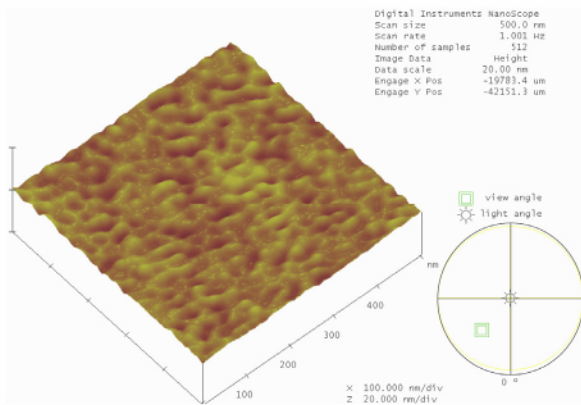

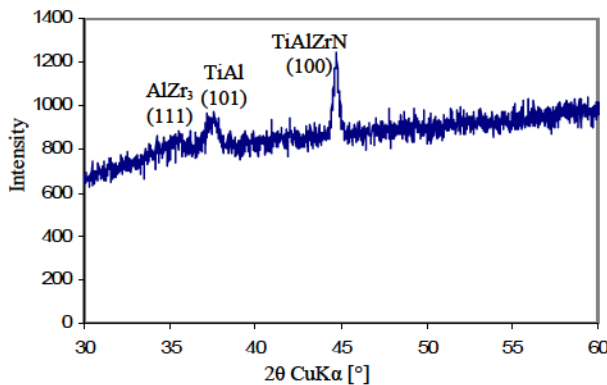Fig. 2. AFM morphologies of surface layer TiAlZrN

Fig. 3. XRD diffractogram of TiAlZrN/TiAlN/TiAl multilayer coating deposited on to AISI4140 steel
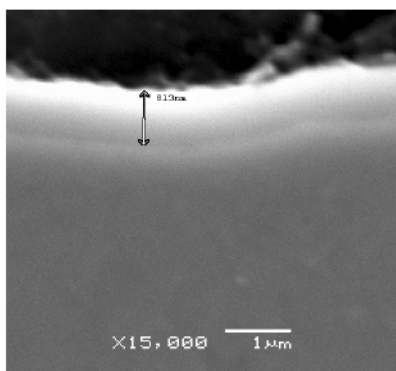

Fig. 4. Scanning electron micrograph of a cross-section of multilayered TiAlZrN/TiAlN/TiAl coating as made by fractography

Dimensional measurements showed that the domes had a mean diameter of about 25nm and the craters a maximum depth of 16nm. The crystallographic structure and orientation of the coatings were determined by x-ray diffraction. Phase identification for multilayer coatings TiAlZrN/TiAlN/TiAl revealed the presence of reflection peaks corresponding to stripes (100) and exhibited a weak intensity peak at $2\theta = 2.83°$ (44.74A°) Fig. 3. It can be seen that the as-coated state already has a crystalline structure of $AlZr_3$. The presence of crystallographic structure is linked to the columnar morphology of the layers observed by SEM on a cross-section Fig. 4.

The chemical composition of multilayered coatings is shown in Fig. 5. The measurements of nanoindentation carried out on a depth exceeding the thickness of the coating made it possible to determine the average hardness and average Young modulus in this multilayer TiAlZrN/TiAlN/TiAl. The results are presented in Table II.
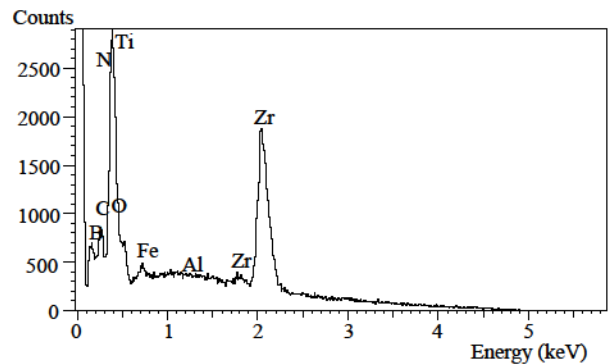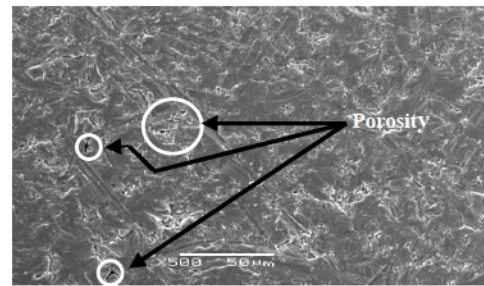

Fig. 5. Energy Dispersive Spectroscopy (EDS) of multilayered TiAlZrN/TiAlN/TiAl coatings

II.4. Fretting Tests

The fretting tests were carried out on an MTS tension compression hydraulic machine.

A sphere-on plane configuration was employed Fig. 6(a). The counter-body was a polycrystalline alumina ball with 24 mm diameter, a Young's modulus 310 GPa and a hardness of 2300 Hv0.05. The flat coating alloy (10mm×10mm×12mm) specimens were manufactured from a cast bar of AISI4140 steel. During the test, the instantaneous displacement, the normal force and the tangential force were monitored and recorded for every cycle.
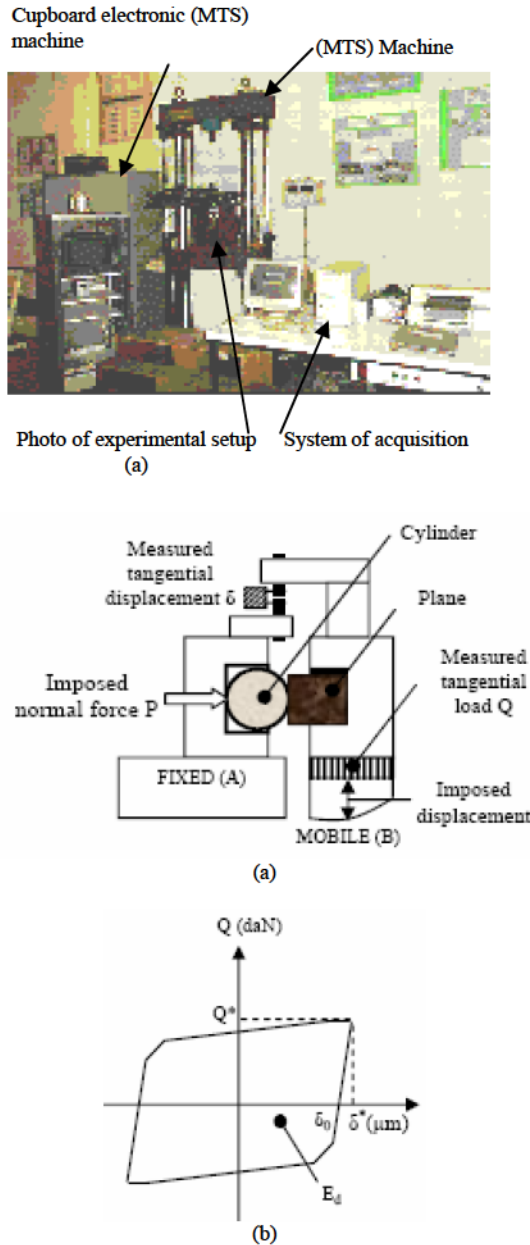
Fig. 6. Illustration of the experimental fretting wear approach:
(a) Photo and schema of the experimental setup;
(b) Fretting log of one fretting cycle

The fretting tests were conducted with displacement control using an extensometer as a displacement transducer. When, it is possible to plot the hysteresis buckles of the fretting cycles from the evolution of the tangential force with displacement for normal force values in the range 50 N to 750 N and displacement from ± 20 μm to ±100 μm. The area of the fretting loop corresponds to the dissipated energy during the fretting cycle (*Ed*), whereas the residual opening of the cycle (i.e. the residual displacement when $Q = 0$) is related to the full sliding amplitude (δ_g) Fig. 6(b). All tests were performed at 20×10^3 cycles and the frequency was set at 5 Hz.

The fretting tests were conducted in dry conditions at an ambient temperature of 25°C and a relative humidity of 60%. Prior to the fretting test, specimen and counter-body were cleaned with acetone and alcohol. Hundred to two thousand fretting cycles were performed. The tests were stopped in two different ways. Once the displacement was stopped abruptly after the last fretting cycle and once the displacement amplitude was reduced to zero during several cycles. However, to quantify the wear volume, a specific 3D surface profilometry methodology fully developed in reference [19] is applied. It consists in determining the wear volume below the reference surface (V⁻) and the transfer volume above the reference surface (V⁺). This analysis is performed both on sphere and plane fretting scars. A system wear volume is then deduced from the following relationship:

$$V_{system} = (V^- - V^+)_{plane} + (V^- - V^+)_{sphere} \qquad (1)$$

However, other conditions have been tested to investigate the effect of certain parameters suspected of having a dominant role in the wear mechanism. These conditions will be given in due course. Furthermore, optical observations are coupled with scanning electron microscopy to examine post test fretting scars.

III. Test Results and Discussion

III.1. Fretting Wear

Preliminary work was carried out to determine the fretting running map of PVD multilayered coatings in contact with alumina sphere. The tangential force (*Q*) and displacement (*δ*) amplitudes are determined for each cycle, and each sliding rate is reported on a 2D map of the fretting displacement and friction force. After a certain number of cycles, the partial-slip regime (PSR) is manifested as a change in the hysteresis loop form, whereas the gross-slip regime (GSR) maintains the buckle form with a variation of tangential force [3]. RCFMs (Running Condition Fretting Maps) can then be determined from this map [16]. Fig. 7 shows the boundary lines of both sliding rates for different multilayered TiAlCN/TiAlN/TiAl and TiAlZrN/TiAlN/TiAl coatings. It can be seen that the gross-slip regime region of the PVD coated AISI4140 steel is enlarged due to the presence of the TiAlZrN then the TiAlCN layers. From a phenomenological consideration, the gross-slip regime corresponds to wear, and in the partial-slip regime, the wear is associated with cracking, the contribution of TiAlZrN/TiAlN/TiAl reducing coatings should be interpreted positively. Indeed, in such a situation, wear is favored with the cracking of the covered part, which makes it possible to sacrifice the surface in order to protect the volume of the part [3].
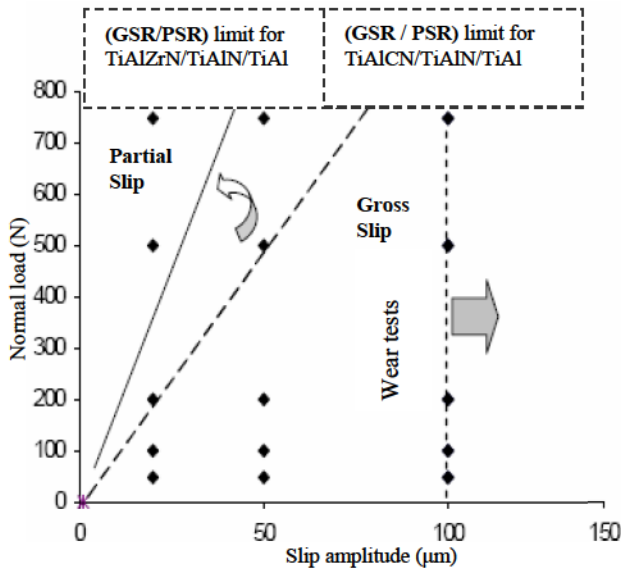
Fig. 7. Effect of multilayered coatings (TiAlZrN/TiAlN/TiAl) on the running condition

The TiAlZrN coating thus reduces the partial-slip regime field, which is the most detrimental for fretting.

However, Sliding amplitudes are rather large and seen to be related more to the reciprocating condition. However, it is fundamental to relate the displacement value to the contact dimension. The boundary between fretting and reciprocating conditions can be related to the ratio between the displacement amplitude and the contact radius, $e = d/a$ [24]. It transpires that when e remains little then 1, a non-exposed surface exists and grosses slip fretting conditions prevail, whereas if e is above 1, the whole surface is exposed to the ambient and the contact is under reciprocating conditions [19]. The maximum e value calculated for all performed test situations remains lower 0.5, which implies gross slip fretting conditions.

III.2. Tribological Properties

Fig. 8 shows the evolution of the coefficient of friction as a function of the total number of cycles for the two multilayered PVD coatings under same loading parameters. The first cycle systematically presents a low friction coefficient around 0.11, the incipient low friction coefficients can be explained by the presence of surface oxides.

During the test, the friction coefficient increases progressively towards a level known as the stabilized friction coefficient. Such a difference of friction behavior between the two antagonists (TiAlZrN and TiAlCN) is clearly illustrated in the graph of evolution of the friction versus the fretting cycles. It confirms the previous fretting cycle analysis and outlines the difference of friction kinetics between the two antagonists.
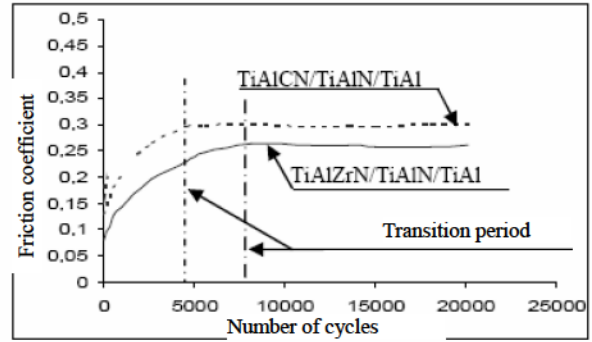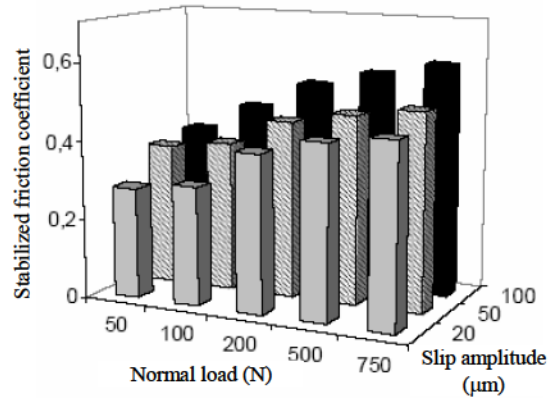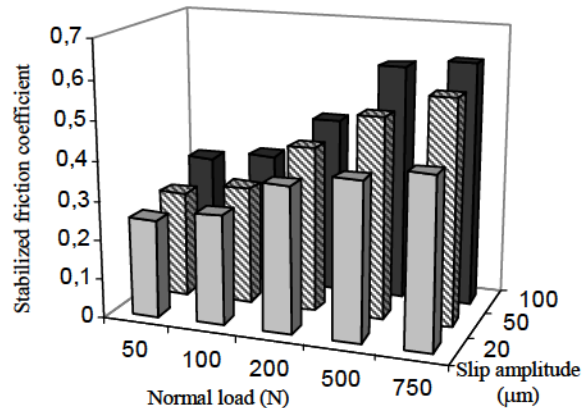

Fig. 8. Evolution of the friction coefficient for the TiAlZrN/TiAlN/TiAl and the TiAlZrN/TiAlN/TiAl ($F_N = 50N$, $\delta = 20\mu m$)

(a)

(b)

Fig. 9. Stabilized friction coefficient as a function of normal load and slip amplitude of PVD multilayered coating (a) TiAlCN/TiAlN/TiAl [3], (b) TiAlZrN/TiAlN/TiAl

The transition period is systematically longer in the presence of the TiAlZrN coating. In the case of the PVD layer, De wit [17] showed that the transition period corresponds to the formation of debris made of amorphous retiles and nanocrystallines. Beyond this transition, the amorphous phase is transformed into a crystalline phase and contributes to further wear.

Depending on the loading condition, the film of TiAlCN or TiAlZrN can be eliminated thus favoring

severe metal/metal surface interactions and yielding a significant increase of the friction coefficient Fig. 9.

It explain the influence of the pressure and displacement amplitude on the evolution of the friction coefficient on a coated specimen taking into account the kinetics of elimination of the low friction top surface must be introduced [18]-[19]. It can be seen that by increasing the displacement amplitude or the pressure the wear depth will grow faster and the elimination of surface porosity will be accelerated. As soon as the surface porosity and the aluminum oxide, which plays the role of a solid lubricant, is removed low friction conditions can no longer be maintained and high metal/metal interactions with high friction coefficients in the range 0.5 to 0.6 are observed indicating that the PVD film has been breached.

When a microarc oxidation coating was used, the fretting friction coefficient of modified PVD coatings alloy under higher loading condition remains as high as about 0.6, however, the cracking domain and severe adhesive was limited. Under low loading condition the friction coefficient was significantly reduced, favorable stable at 0.4 - 0.3 in the long-term, which indicates that the multilayered coatings lowered the shear and adhesive stresses between contact surfaces, consequently alleviating the possibility of initiation and propagation of cracks in the inner layer of multilayered coatings.

III.3. Wear Properties

In every tribological application, the extent of the damage or surface deterioration is of interest. There are several methods of evaluating the wear volume/loss, which can be roughly classified into three methods weight measurement, topographical analysis and 2D analysis by means of empirical equations. In tribological research where many specimens need to be analyzed, a simple and fast procedure is desirable for wear volume/ loss determination. Moreover, the effect of different material combinations, slip amplitude, normal force, and the energy dissipated during sliding, is also presented.

III.3.1. Prediction of the Wear Volume Evolution

The linearity of the variation of fretting wear with normal load and displacement obtained by the two multilayered TiAlCN/TiAlN/TiAl and TiAlZrN/TiAlN/TiAl coated specimens are used to impose the same definition as Archard's equation, namely a quasi linear function. The wear volume evolution of the two coated steels is shown in Fig. 10, as a function of slip amplitude and normal force. For all specimens, the beneficial effects of the coating on wear volume diminished with increasing normal force, and fretting stroke. The latter observation is consistent with the work of Santner et al. [20], who reported that TiN

was much more effective at suppressing wear under sliding wear conditions. For the steel substrate, the coating TiAlCN or TiAlZrN had no good effect on fretting wear for sliding amplitudes larger than 50μm, regardless of the applied normal forces out of 500N. The wear transition is attributed to the higher variation of both normal load and sliding amplitude.

However, for all fretting-wear tests the behaviour evolution of wear volume versus displacement is the same. This means in all tests, wear volume remain constant and are not greatly influenced by low normal load or sliding distance. In fact, is only the wear amplitude which changes according to displacement and high normal load. In every case, there is a constant wear volume which precedes the establishment of the high wear regime. Three suppositions can be made to synthesise all the results presented above.

Wear volume are similar for all loading conditions, and consist of two phases. The first one corresponds to the elimination of the contamination layer and the natives oxides. Thus, Alumina to PVD coatings contact will be established. As a result the adhesion phenomenon is favoured as regards the miscibility antagonists by plastic deformation, which increases micro-junction density by crushing asperities. Hence adhesive wear appears by creating transfer of the softer material (PVD coatings) on the harder material (alumina). This phase will be followed by a transitional stage: wear transferred PVD coatings.

The second phase (high wear regime) happens as soon as the trapped debris is oxidised. Gradually, wear is accentuated on both sides of contact (on PVD coatings and alumina ball). For larger displacements ($\delta >$ 50μm) and a high normal load, fatigue wear induced by multicracks has been detected Fig. 11. One hypothesis is that the generated plastic strain leads to a brittle layer, which can be associated to the tribologically transformed structure (TTS) [25]-[26]. Enduring cyclic loading multicracks are activated which induce debris formation and wear.
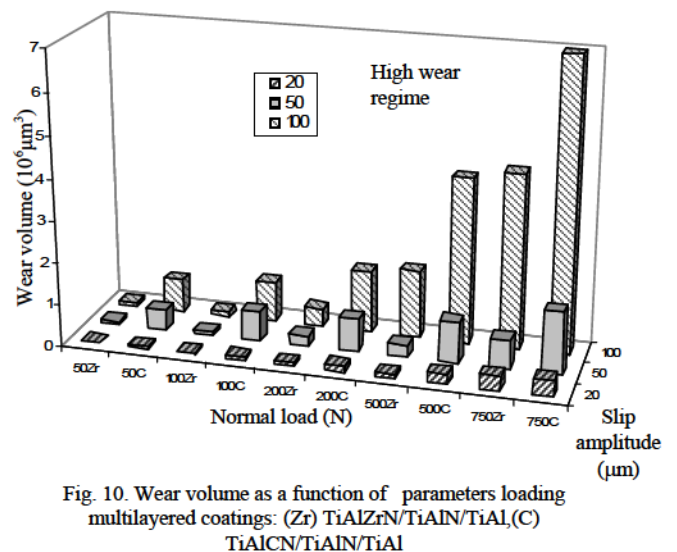

Fig. 10. Wear volume as a function of parameters loading multilayered coatings: (Zr) TiAlZrN/TiAlN/TiAl,(C) TiAlCN/TiAlN/TiAl
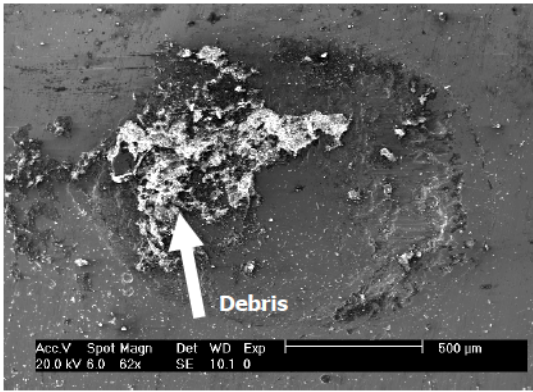
Fig. 11. Fretting wear scar morphology of multilayered TiAlZrN/TiAlN/TiAl coating (Gross Slip Regime), $F_N = 200N.\delta = \pm 100\mu m$

The main wear mechanism of TiAlZrN coated AISI4140 steel was the brittle cracks of TiAlZrN before destroying the coating. After destroying the TiAlZrN coating, the main wear mechanism was cracks due to a low normal force and high slip amplitude and cumulated plastic flow on the edge of the fretting scar and adhesive and abrasive wear at high slip amplitude. Oxidation was observed on most the worn surface.

III.3.2. Prediction Energy Wear Coefficient

Investigations at various loads and slip amplitudes confirm that there exists a correlation between the wear volume extension of TiAlZrN/TiAlN/TiAl multilayer coating and dissipated energy. For all the different loading conditions previously defined in the paragraph (2.4), Fig. 12 shows the rates of the wear volume as a function of the dissipated energy. As distinct form this behavior, when the energy approach is applied all the loading conditions are represented by one and only linear platform from which a unique global energetic wear coefficient (α) can be derived. In the case under consideration $\alpha_{TiAlZrN} = 10^4 \mu m^3/J$, and TiAlCN coating provides an energetic wear coefficient of $\alpha_{TiAlCN} = 23.10^3 \mu m^3/J$ [3].
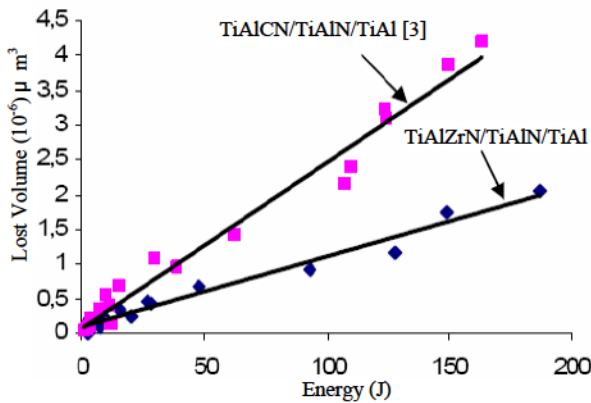

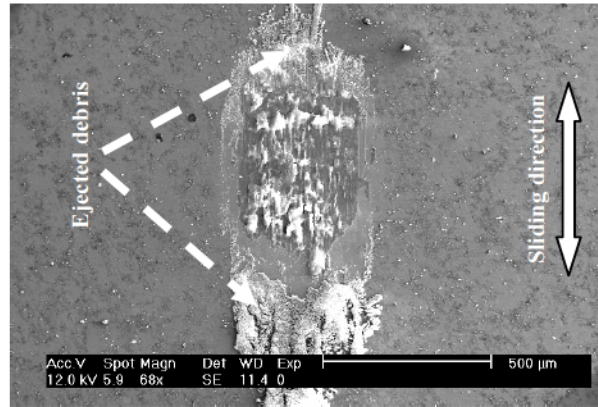Fig. 12. Wear volume as a function of cumulated dissipated energy

Fig. 13. Fretting wear scar morphology of multilayer TiAlZrN/TiAlN/TiAl coating (Partial Slip Regime)

This result shows that the TiAlZrN coating improves its higher capacity to wear in fretting. The principal factors favoring this tendency are generally related to the presence of compression residual stress, the decrease of friction coefficient, the increase of superficial hardness, and the roughness effect of the surface [21]. Without measuring the residual stress, the contribution of the reduction of friction coefficient and the increase in hardness are confirmed in this study.

One can notice as in Fig. 13 that hard coatings quickly give rise to particle detachment and prevent the partial slip regime by accommodating the displacement in the powder bed and favors debris formation. A large amount of debris has been observed during fretting tests and coatings are damaged by material transfer due to adhesion and/or abrasion. It can be seen that a small amount of debris remains within the contact area, while large amount of debris is ejected outside and located near to the border of the fretting scar.

However, fretting scars have three characteristic regions, which are clearly visible for multilayered TiAlZrN/TiAlN/TiAl coating; central convex region with slight abrasion traces, outer annular region covered with debris and transition region where the abrasion traces parallel to the sliding direction can be easily identified.

Fig. 14 compares the energetic wear coefficients with those reported in the literature [3], [21], [22]. Magnetron sputtered TiAlZrN coatings in the as-deposited condition possess a better fretting wear resistance ($10^4 \mu m^3/J$) than TiAlCN coatings ($23 \mu m^3/J$) for tests performed in ambient air. According to energetic considerations, the multilayered TiAlZrN coatings improve the resistance to fretting wear by a factor 6.5, compared with non-coated steel [3]. But the TiAlCN multilayer has a lower performance as it improves the resistance only by a factor of 2.8. This result is acceptable since the addition of Al, Zr forms stable oxides, especially Zr forms a very thin oxide layer similar to Al_2O_3 [5], [22], [23] that strongly influences the energetic wear coefficient, and provides good tribological properties [5].
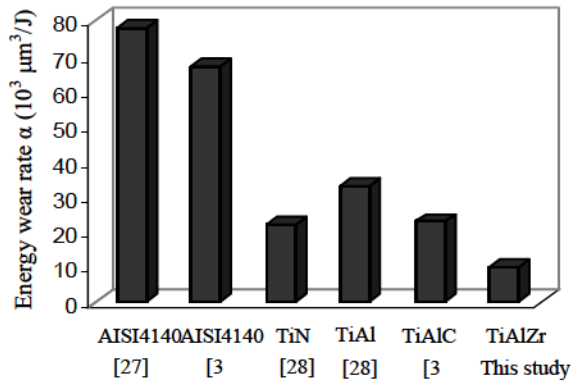
B. Tlili, M. Nasri, F. Ayari, C. Nouveau

Fig. 14. Energy wear rates of different substrates and hard coatings in fretting wear tests

IV. Conclusion

In this work, we reviewed deposition parameters and properties of titanium and titanium-aluminum based quaternary coatings. It is found that the effect of individual as well as multiple alloying elements are manifested in further modifying the properties of (Ti, Al) N coatings. Research and developments on simple binary and ternary coatings in previous studies are discussed. This was followed by the investigations on quaternary multicomponent coatings (TiAlZrN/TiAlN/TiAl and TiAlCN/TiAlN/TiAl); the behaviours in these coatings in fretting wear are compared. The main conclusions are the following.

The local card solicitation obtained for the two layers quaternary studied, shows the delimitation of both sliding rates. It is shown that the gross-slip regime region (GSR) of the coated AISI4140 steel is extended by the presence of the TiAlZrN layer in comparison with the TiAlZrN layer. These results are being very useful in the tribology. Indeed, the GSR is always associated to wear, but the partial slip regime (PSR) is accompanied to a crack that can be disastrous and leads to the failure.

To reduce the instantaneous friction coefficient and stabilized friction coefficient, it is necessary to choose the coating based zirconium coating instead of the coating based carbon. However, the gap between these two coating is governed by the amplitude of the loading parameters. The thin coatings formed by physical vapour deposition may provide an initial friction reduction but it is not sufficiently durable for this application. However, the beneficial effect of the PVD coatings on fretting wear diminishes with increasing normal force and decreasing fretting stroke.

In this paper the worn volume of the two quaternary layers is very influenced by loading conditions. Therefore, special attention should be given to better distinguish the effect of zirconium. Adding Zr improves the wear resistance of Al-Ti-N coating. Zr stabilizes Ti-Al-N lattice and also forms a very thin stable oxide layer similar to Al_2O_3. These two effects together enhance the wear resistance of Ti-Al-Zr-N coatings.

The stability of the energy approach is used to predict the wear kinetics in a volume of tribo-systems:

$$Wv = \alpha \times \sum Ed$$

where, α: is the energetic coefficient, Wv: worn volume, Ed: dissipated cumulated energy.

The multilayered TiAlZrN/TiAlN/TiAl coatings improve the resistance to fretting wear of AISI4140 steel of twice as much as the multilayered TiAlCN/TiAlN/TiAl coatings.

References

[1] Nanastructured coatings for high performance tools (PLATIT). Werkzeug Technik, 2003, 77, March.
[2] PalDey, S. and Deevi, S. C. Single layer and multilayer wear resistant coatings of (Ti, Al) N: a review, Mater. Sci. Eng. A, 2003, 342, 58-79.
[3] A. Ben Cheikh Larbi, B. Tlili, Surf. Coat. Technol. 257-8972(2006) 167-168.
[4] D.-F. Lii, J-L. Huang, M. H.-H. Lin, Surf. Coat. Technol. 99 (1998) 197.
[5] S. PalDey, S.C. Deevi, Materials Science and Engineering A342 (2003) 58-79
[6] S. Fouvry, Ph. Kapsa, L. Vincent, A global methodology to quantify fretting damage, in : Y. Mutch, S.E.Kiyon, D. W. Hoeppner (Eds.), Fretting Fatigue: Advances in Basic Understanding and Applications, STP 1425, American Society for Testing and Materials, West Conshohocken, PA, 2033, pp. 17-32.
[7] S. Fouvry, Ph. Kapsa, L. Vincent, Wear 185 (1995) 35-46.
[8] S. Fouvry, K. ELLeuch, G. Simeon, J. Strain Anal. 37 (6) (2000) 703-716
[9] H. Proudhon, S. Fouvry, G.R. Yantio, Int. J. Fatigue 28 (2006) 707-713
[10] H.C. Meng, K.C. Ludema, Wear 181-183 (1995) 443-457.
[11] E. Lugscheider, O. Knotek, C. Barimani, T. Leyendecker, O. Lemmer, R. Wenke, surf. Coat. Technol. 112 (1999) 146-151.
[12] M. Godet, The third body approach, Wear 100 (1984) 325-437.
[13] S. Descartes, C. Desrayaud, E. Nicollini, Y. Berthier, Wear 258 (2005) 1081-1090.
[14] Y. Berthier, L. Vincent, M. Godet, Wear 125 (1998) 25-38.
[15] H. Mohrbacher, B. Blanpain, J.P. Celis, J.R. Roos, L. Stals, M. Van Stappen, Wear 188 (1995) 130-137.
[16] M.C. Dubourg, A.Chateauminois, B.Villechaise, Tribology International 36 (2003) 109-119.
[17] E. Dewit, B. Blanpain, L. Froyen, J.P. Celis, wear 217 (1998) 215-224.
[18] F. P. Bowden, D. Tabor, Friction and lubrification of solids, vol.1, Oxford University Press, London, 1964.
[19] K. Elleuch, S. fouvry, Wear 253 (2002) 662-672.
[20] E. Santner, D. Klaffke, G.M.Z. Kocker, Wear 190 (1995) 204-211.
[21] K. Holmberg, A. Matthewst, H. Ronkainen, Tribology International Vol 31, Nos 1-3 (1998) 107-120.

[22] O. Knotek, W. D. Münz, T. leyendecker, J. Vac. SCi. Technol. A5 (4) (1987) 2173-2179.
[23] O. Knotek, M. Böhmer, T. Leyendecker, F. Jungblut, Mater. SCi. Eng. A105-106 (1988) 481-488.
[24] S. Fouvry, P. Kapsa, L. Vincent, Wear 200 (1-2) (1996) 186-205.
[25] E. Sauger, S. Fouvry, L. Ponsonnet, Ph. Kapsa, J.M. Martin, L. Vincent, Wear 245 (2000) 39-52.
[26] E. Sauger, L. Ponsonnet, J.M. Martin, L. Vincent, Tribol. Int. 33 (2000) 743-750.
[27] M. Varenberg, G. Halperin, I. Etsion, Wear 252 (2002) 902.
[28] B. Prakash, C. Ftikos, J.-P. Celis, Surf. Coat. Technol. 154 (2002) 182.

Authors' information

[1]MAII, Ecole Nationale d'Ingénieurs de Tunis,
BP 37 Le belvedere 1002 Tunis,
Tunisia
Institut Préparatoire aux études d'Ingénieurs el Manar
2092 el Manar- B.P .244
Tunis.
Tel./Fax: 216 71 874 688 / 216 71 873 948
E- mail: tlilii_brahim@yahoo.fr

[2]LMSDT, Ecole Superieur des Sciences et Technique de Tunis,
1008 Montfleury, Tunis,
Tunisia.

[3]Laboratoire Bourguignon des Matériaux et Procédés,
Rue porte de Paris 71250 Cluny,
France.

International Review of
Mechanical Engineering
(IREME)

Authors

Praise Worthy Prize